

Island of Rare Earth Nuclei with Tetrahedral and Octahedral Symmetries: Possible Experimental Evidence

J. Dudek,¹ D. Curien,² N. Dubray,¹ J. Dobaczewski,³ V. Pangon,¹ P. Olbratowski,³ and N. Schunck⁴

¹*Institut Pluridisciplinaire Hubert Curien IN2P3-CNRS/Université Louis Pasteur, F-67037 Strasbourg Cedex 2, France*

²*Institut Pluridisciplinaire Hubert Curien IN2P3-CNRS, F-67037 Strasbourg Cedex 2, France*

³*Institute of Theoretical Physics, Warsaw University, Hoza 69, PL-00681 Warsaw, Poland*

⁴*Departamento de Fisica Teorica, Modulo C-XI, Universidad Autonoma de Madrid, Cantoblanco 28049 Madrid, Spain*

(Received 13 March 2006; published 15 August 2006)

Calculations using realistic mean-field methods suggest the existence of nuclear shapes with tetrahedral T_d and/or octahedral O_h symmetries sometimes at only a few hundreds of keV above the ground states in some rare earth nuclei around ^{156}Gd and ^{160}Yb . The underlying single-particle spectra manifest exotic fourfold rather than Kramers's twofold degeneracies. The associated shell gaps are very strong, leading to a new form of shape coexistence in many rare earth nuclei. We present possible experimental evidence of the new symmetries based on the published experimental results—although an unambiguous confirmation will require dedicated experiments.

DOI: 10.1103/PhysRevLett.97.072501

PACS numbers: 21.10.-k, 21.60.Fw, 27.70.+q

Symmetries of molecules, fullerenes, metal clusters, atomic nuclei, and many other quantum objects can be conveniently described with the help of group theory that provides a powerful means of classifying spectra in terms of the group representations. The symmetries of, for instance, Fermion mean-field Hamiltonians, are described with the help of double point groups whose irreducible representations determine the degeneracies of spectra and thus the underlying shell structure. Among all known double point groups, only three, i.e., tetrahedral, T_d (“pyramid”), octahedral, O_h (“diamond”), and icosahedral (I_h) lead to “exotic” fourfold degeneracies of single-Fermion levels; all other symmetries lead to twofold degeneracies only. This high-degeneracy aspect leads to high stability of implied nuclear shapes, as it turns out, Ref. [1]. The symmetry plays a unifying role among distinct fields: in particular, experiments show that in the alkali metal clusters the observed magic numbers are 40, 70, and 112 (cf., e.g., Ref. [2] and references therein) while Ref. [1] predicts those (as well as some other) magic numbers for the atomic nuclei.

While an accidental discovery of the C_{60} fullerene, one of the “most symmetric” objects in nature, took place over 20 years back, it remains to hope that an unambiguous experimental discovery of the most symmetric (tetrahedral and/or octahedral) nuclei will follow soon.

A possible existence of nuclei with exotic shapes that resemble round-edge pyramids (tetrahedral symmetry) has been a subject of a number of publications addressing so far mainly the theoretical aspects. In particular, Ref. [3] discussed for the first time the underlying fourfold degeneracies of single-particle levels in nuclei. In Ref. [1] group-theory aspects of tetrahedral symmetry in nuclei have been presented and existence of “tetrahedral” magic numbers suggested. These numbers correspond to particularly large gaps in the nucleonic single-particle spectra related to the

pyramidlike shapes. Calculations show that there exist magic tetrahedral gaps in many areas of the periodic table. Using the self-consistent Hartree-Fock approach solutions with the tetrahedral symmetry in light nuclei have been obtained in Ref. [4]. In the more recent Ref. [5], it has been pointed out that some exotic nuclei around ^{110}Zr may be tetrahedral symmetric in their ground states.

In this Letter we address the question of stable nuclear configurations with tetrahedral and octahedral symmetries corresponding to the groups of symmetry of tetrahedron, T_d , and cube, O_h , respectively. They belong to the groups of symmetry of regular polyhedra—the richest in terms of symmetry operations—among the point groups currently used in physics. Any surface invariant with respect to all of those operations is called T_d invariant. The corresponding nucleonic mean-field Hamiltonian is invariant with respect to the double T_d group, denoted T_d^D , composed of 48 symmetry elements.

We performed systematic calculations for several hundreds of nuclei with $60 \leq Z \leq 76$, using the standard Strutinsky method with the Yukawa-folded macroscopic energy parametrization of Ref. [6] and the mean-field approach with the deformed Woods-Saxon (WS) potential

$$V(\vec{r}; \{p\}) = \tilde{V}(N, Z) / \{1 + \exp[\text{dist}_\Sigma(\vec{r}; r_0)/a]\}. \quad (1)$$

Above, $\{p\}$ denotes the ensemble of the central potential Z - and N -independent parameters, r_0 , a , V_0 , and κ , whereas $\tilde{V}(N, Z) \equiv V_0[1 \pm \kappa(N - Z)/(N + Z)]$; see Ref. [7] for details. The WS spin-orbit potential has the standard form of $V_{\text{so}}(\vec{r}; \{p\}_{\text{so}}) \equiv (\vec{\nabla}V \wedge \hat{p}) \cdot \hat{s}$, where \hat{p} and \hat{s} are the linear momentum and spin operators, respectively, and $\{p\}_{\text{so}}$ denotes the ensemble of the spin-orbit potential parameters analogous to those of the central one. In the calculations the universal parameter set of Ref. [7] has been used together with a totally new parametrization

obtained by fitting the single-particle levels, nucleonic binding energies and proton (neutron where known) root-mean-square radii to the currently known experimental data [8]. The results of both parametrizations are similar; the new one has been chosen for illustrations in this Letter.

These calculations have been cross-checked with the help of the Hartree-Fock-Bogolyubov (HFB) method [9], using three types of the Skyrme interactions: SIII, SkM*, and SLy4 and the contact pairing force. All results point clearly to strong shell effects associated with the tetrahedral symmetry in rare earth nuclei.

As it turns out, examining the octahedral symmetry will be important to learn more about the tetrahedral symmetry in nuclei. Octahedral group O_h has 48 symmetry elements and the related double point group O_h^D of the mean-field Hamiltonian contains in total 96 symmetry elements. Both the tetrahedral- and octahedral- invariant surfaces can be modeled with the help of the standard spherical harmonic expansion

$$R(\vartheta, \varphi) = R_0 c(\{\alpha\}) \left[1 + \sum_{\lambda} \sum_{\mu} \alpha_{\lambda\mu} Y_{\lambda\mu}(\vartheta, \varphi) \right] \quad (2)$$

by selecting appropriately a subset of spherical harmonics that are allowed by a given symmetry.

By requiring that expression (2) is invariant under T_d one obtains the following conditions for odd λ : the lowest-order parametrization corresponds to $\alpha_{\lambda\mu} = \alpha_{32}$; there is no 5th order while the 7th order satisfies $\alpha_{7,\pm 2} \equiv t_7$ with $\alpha_{7,\pm 6} = -\sqrt{11/13}t_7$. Similarly, invariance under O_h implies that only even λ is allowed, and one may have $\alpha_{40} = o_4$ and $\alpha_{4,\pm 4} \equiv -\sqrt{5/14}o_4$ in the 4th order, and $\alpha_{60} \equiv o_6$ and $\alpha_{6,\pm 4} \equiv -\sqrt{7/2}o_6$ in the 6th order.

Since T_d is a subgroup of O_h , subsets of spherical harmonics representing the T_d and O_h symmetries listed above can be combined into surfaces having again the T_d symmetry. As a consequence, these combinations form the lowest-order T_d symmetry basis that can be used in multi-dimensional searches for the nuclei with tetrahedral symmetry minima. Examples of such potential energy surfaces are given in Fig. 1 for ^{156}Gd . In this nucleus, the total energy at tetrahedral minimum is lower by 2.88 MeV compared to the spherical shape, and 3.15 MeV above the quadrupole minimum. The barrier separating the two minima amounts to about 0.75 MeV.

A summary of similar results for nuclei in the rare earth region is given in Figs. 2 and 3. Differences between the Strutinsky nuclear energies at spherical and tetrahedral shapes (ΔE_{ST}) shown in Fig. 2 (left) illustrate the importance of the shell effects that drive the nuclei towards the tetrahedral symmetry. The predicted effects increase with the neutron numbers and approach ~ 5 MeV at $N \sim 102$. At the same time, differences between the energies at tetrahedral and prolate shapes (ΔE_{TP}) shown in Fig. 2 (right) also increase, while the barriers between the tetra-

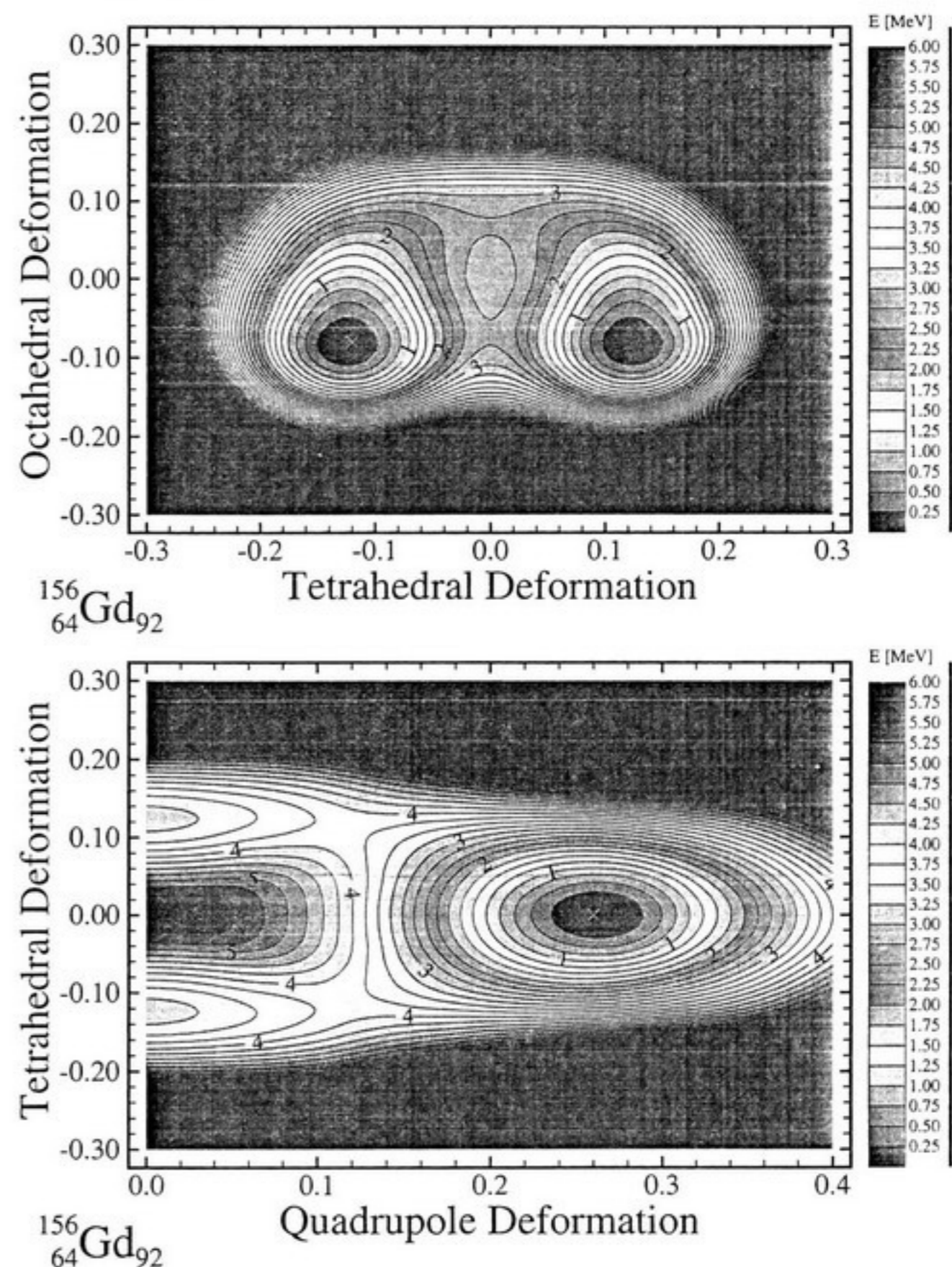


FIG. 1 (color online). The total Strutinsky energy of ^{156}Gd nucleus in function of the lowest-order ($t_3 \equiv \alpha_{32}$) and octahedral (o_4) deformations shown at $\alpha_{20} = 0$ (top) and in function of the quadrupole (α_{20}) and tetrahedral (t_3) deformations, with each point of the plane minimized with respect to o_4 (bottom).

hedral and prolate shapes decrease, as shown in Fig. 3. Still, in many gadolinium ($Z = 64$) and ytterbium ($Z = 70$) nuclei these barriers are of the order of several MeV, values sufficient to expect measurable effects. Observe a grouping of several high barriers corresponding to the $N = 90, 92$ isotones. All in all, light isotopes of these two elements are probably the best candidates to observe relatively stable and not-too-much excited tetrahedral configurations in experiment.

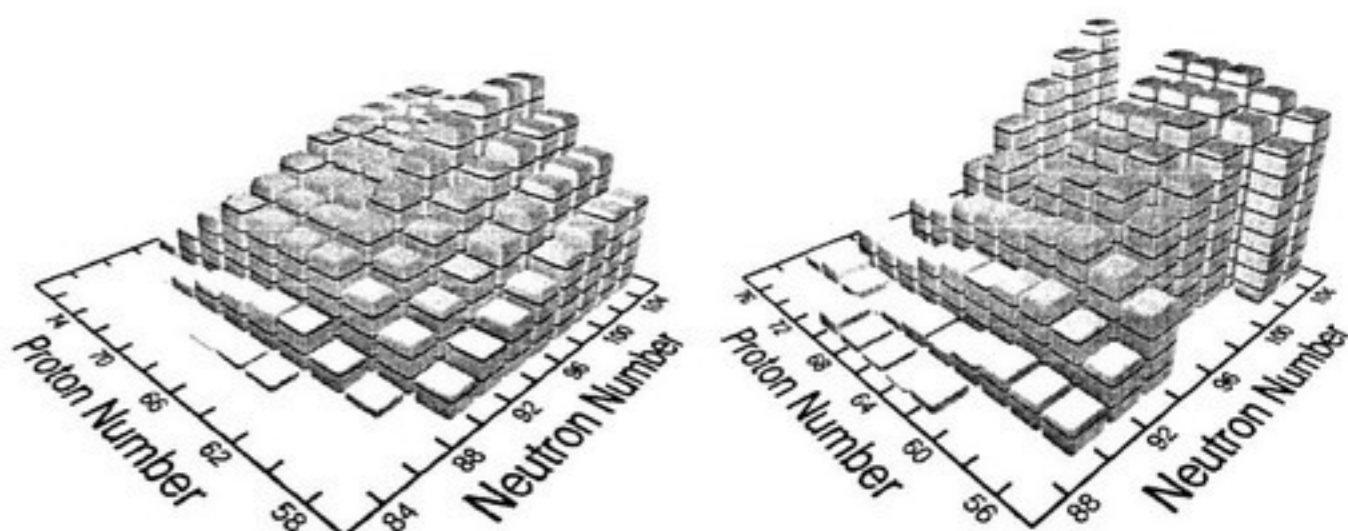


FIG. 2. Energy differences between the spherical and tetrahedral (left) and tetrahedral and prolate (right) shapes. Each brick in the stack represents 500 keV (left) and 1 MeV (right).

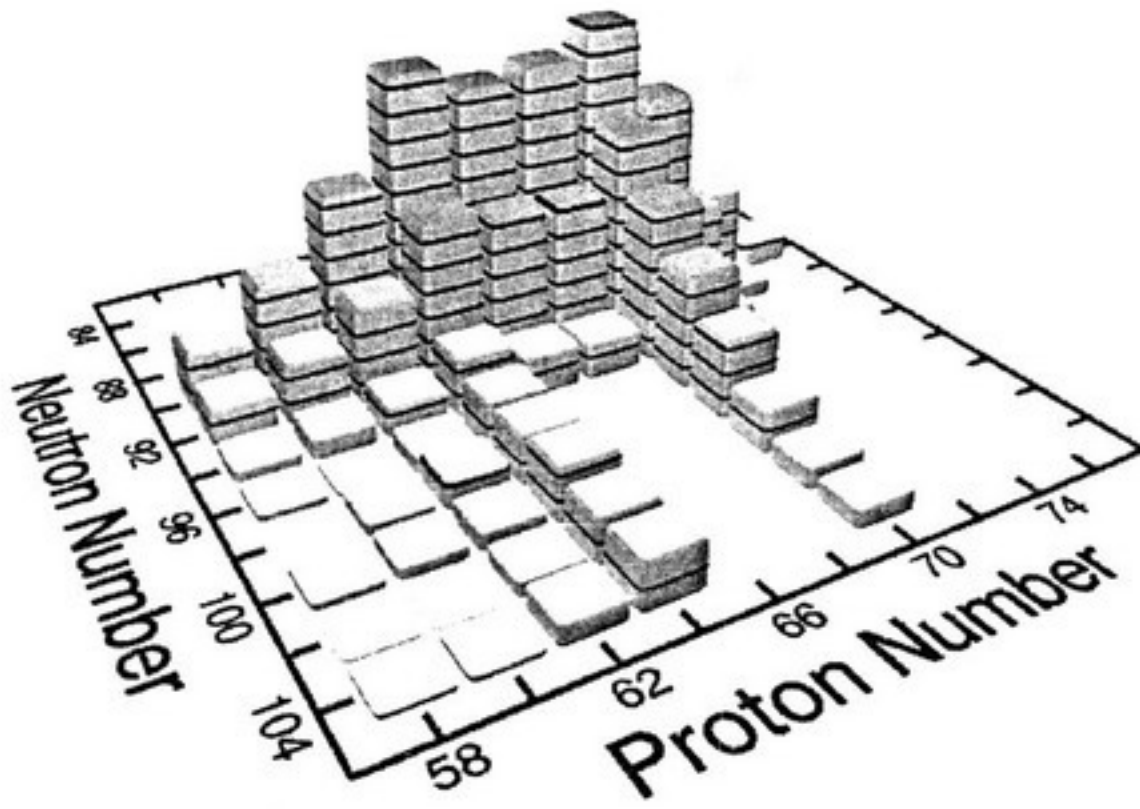


FIG. 3. Barriers between tetrahedral and quadrupole minima (cf. Fig. 1 bottom). Each brick in the stack represents 100 keV.

The Skyrme-HFB results for three gadolinium isotopes obtained by using the code HFODD (v2.20m) [9] are given in Table I. Calculations were performed for the harmonic-oscillator basis of 16 spherical shells, and for the proton and neutron pairing strengths adjusted to reproduce the experimental pairing gaps in $^{156}\text{Gd}_{92}$. For comparison, Table I also shows the Strutinsky results obtained for the WS potential. In general, the shell effects obtained within the Skyrme-HFB method at tetrahedral (prolate) shapes are weaker (stronger) than those of the Strutinsky method. Moreover, at variance with the Strutinsky calculations, the HFB results show only a rather flat regions of the potential energy surfaces near the tetrahedral shapes that turn out to be unstable with respect to the quadrupole deformation. However, typical Skyrme parametrizations used in the present study do not have good enough spectroscopic-quality predictive power and better fine-tuned parametrizations should be found to be more realistic in the present context.

We believe that the experimental signals of the phenomenon in question may already be present in the existing experimental data. As an example, in Fig. 4 we show two rotational bands in ^{156}Gd [10]. For $I \leq 9$, the existence of the negative-parity band, $I^\pi = 19^- \rightarrow 17^- \dots \rightarrow 5^- \rightarrow 3^-$, is known only through the interband dipole transitions, the intraband $E2$ transitions being totally absent in over a dozen of experiments that reported the band in question.

TABLE I. Energy differences (in MeV) between the spherical and tetrahedral (ΔE_{ST}) and tetrahedral and prolate (ΔE_{TP}) shapes obtained within the Skyrme-HFB and Strutinsky methods.

Nucleus	ΔE_{ST}				ΔE_{TP}			
	SIII	SkM*	SLy4	WS	SIII	SkM*	SLy4	WS
$^{152}\text{Gd}_{88}$	0.25	0.48	0.17	1.06	3.01	2.27	3.16	0.19
$^{154}\text{Gd}_{90}$	0.79	1.38	0.67	2.37	5.31	4.29	5.36	0.81
$^{156}\text{Gd}_{92}$	1.29	1.54	0.94	2.88	7.72	7.27	7.95	3.15

Similar bands are also known in a number of nuclei near ^{156}Gd .

In our opinion, the puzzling feature of a negative-parity $\Delta I = 2$ band having no, or very weak, $E2$ transitions can be explained by the tetrahedral shape of the rotating nucleus. In order to substantiate such a hypothesis, let us briefly discuss expected properties of the rotational bands associated with tetrahedral minima. The dipole and quadrupole moments of a nucleus possessing the exact T_d symmetry are equal to zero, and thus the corresponding electric radiation would be limited to octupole $E3$ transitions. This is in contrast with the “usual” pear-shape octupole deformation superposed with a sizeable quadrupole deformation leading to strong $E2$ and $E1$ transitions. However, let us emphasize that an ideal static-tetrahedral-symmetry picture needs to be modified when we wish to address, even semiquantitatively, the problem of radiation. As it is known from the standard electric-radiation proba-

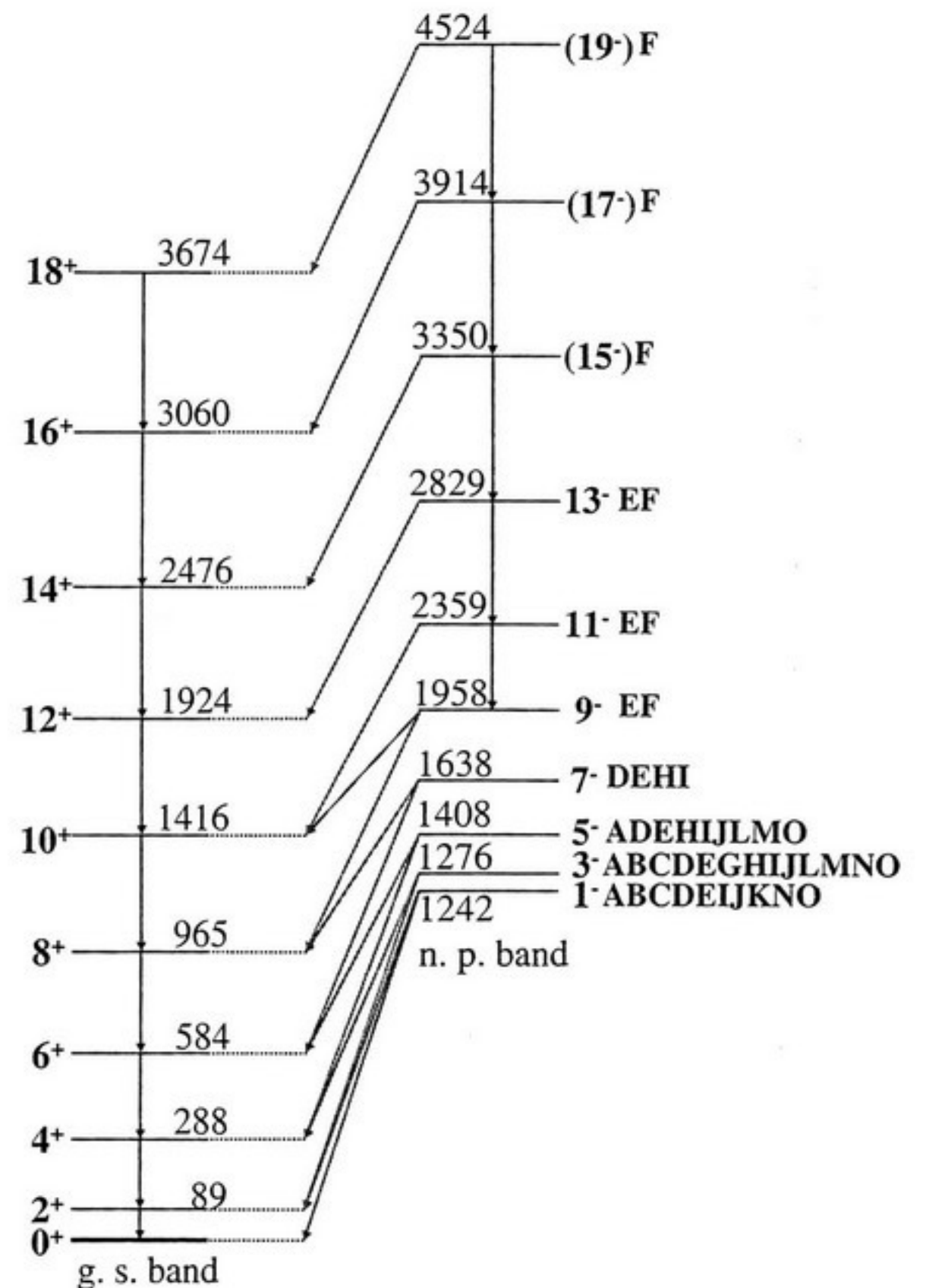


FIG. 4 (color online). Partial decay scheme of ^{156}Gd nucleus showing the negative-parity band connected to the yrast band through $E1$ transitions. The low-spin $E2$ transitions from 9^- to 1^- were never observed although numerous and very different population methods have been used; in fact the letters next to the levels refer to the experimental papers according to the code of Ref. [10], where the original references can be found. Energy wise the state $I^\pi = 1^-$ does not belong to the parabolic $I(I+1)$ sequence, lying 77 keV above the otherwise regular parabola, neither it is expected to belong to the tetrahedral (thus $K^\pi = 2^\pi$) band.

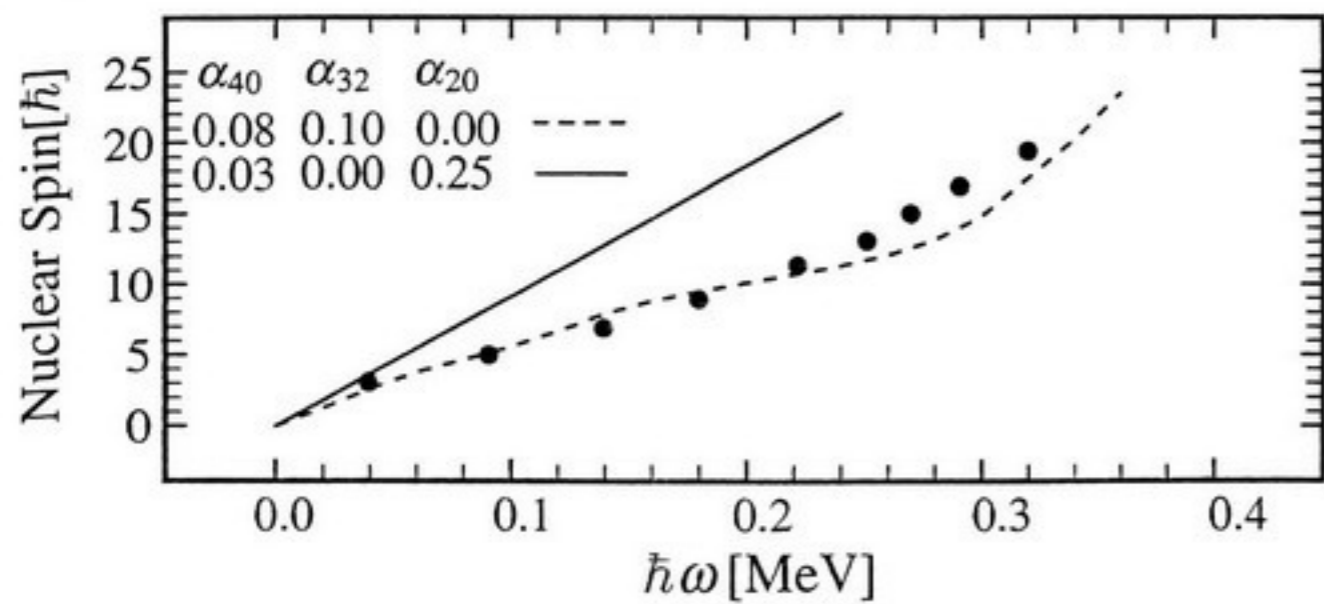


FIG. 5. Nuclear spin in function of rotational frequency, full dots give experimental results of Ref. [10]. Dashed line: octahedral deformation $\alpha_4 \leftrightarrow \alpha_{40} = 0.08$ superposed with $\alpha_3 \equiv \alpha_{32} = 0.10$ tetrahedral deformation from the energy minimization.

bility formulas, the transformation from the reduced transition probabilities to probabilities involves large factors such that the $E1$ transitions very easily win the competition with the $E3$'s. Thus the presence of relatively small dipole polarizations, induced by rotation and/or zero-point motion, makes the corresponding transitions orders of magnitude stronger than the unmasked $E3$'s related to tetrahedral deformation.

The quadrupole zero-point vibration around the tetrahedral shape may indeed lead to a nonzero mass (and charge) dipole moment $Q_{\lambda\mu}$ for $\lambda = 1$. Within a simple geometrical picture of the nuclear surface described by Eq. (2), we have $Q_{10} \simeq 9/\sqrt{21}\pi \times \rho_0 R_0^4 \alpha_{3\pm 2} \alpha_{2\pm 2}$, where the tetrahedral (α_{32}) and dynamic quadrupole ($\alpha_{2,2}$) deformations are assumed to be small. Of course, the final value of the electric dipole moment results from a balance between the mass and charge deformations and can only be estimated within a true microscopic calculation. However, the argument helps to understand qualitatively the presence of the dipole transitions and unobservably small quadrupole transitions in hypothetical tetrahedral bands of nuclei such as ^{156}Gd .

Figure 5 illustrates the alignment curves for ^{156}Gd at the tetrahedral and octahedral deformations, respectively, $\alpha_{32} = 0.1$ and $\alpha_4 \leftrightarrow \alpha_{40} = 0.08$, as obtained by our multi-dimensional calculations, compared to quadrupole deformation typical for the ground-state minimum $\alpha_{20} = 0.25$ and $\alpha_{40} = 0.03$. We conclude that at low-spin range the experimental moments of inertia should take roughly 30% to 40% lower values compared to the ground-state moments of inertia.

The likely features of the tetrahedral rotational bands are as follows: (i) due to their octupole character they are of negative parity, (ii) because of the relatively small values of the (induced) quadrupole moments the intraband $E2$ transitions are expected to be weak, (iii) following our calcu-

lations they are expected to lie above the ground state some hundreds keV to a few MeV around ^{156}Gd and ^{160}Yb nuclei, (iv) the dipole interband transition probabilities from the bands in question to the ground-state bands are expected to be markedly larger as compared to the intraband $E2$ transition probabilities, especially at the bottom of the tetrahedral bands. We may expect that experimental results may contain only the interband $E1$ transitions due to the side feeding of the tetrahedral bands—and weak or no $E2$ transitions at all.

In summary, the possible presence of the tetrahedral and octahedral symmetries in rare earth nuclei around ^{156}Gd and ^{160}Yb nuclei is predicted following the microscopic calculations using realistic nuclear mean-field methods. Predicted properties of the bands are discussed and compared with one of the band candidates in ^{156}Gd nucleus. In order to unambiguously identify the presence of the tetrahedral symmetry, the branching ratios of the related bands should be measured with sufficient precision. On the theoretical side, calculations of the induced dipole moments and transitions in the regime of small deformations should be undertaken and mean-field parametrizations should be fine-tuned to account for experimental positions of the hypothetical tetrahedral bands.

This work was supported in part by the Polish Committee for Scientific Research (KBN) under Contract No. 1 P03B 059 27 and by the Foundation for Polish Science (FNP). This work is a part of activities of the collaboration TETRANUC, whose support through the IN2P3, France, is acknowledged.

-
- [1] J. Dudek, A. Gózdź, N. Schunck, and M. Miśkiewicz, Phys. Rev. Lett. **88**, 252502 (2002).
 - [2] S. M. Reimann, M. Koskinen, H. Häkkinen, P. E. Lindelof, and M. Manninen, Phys. Rev. B **56**, 12 147 (1997).
 - [3] X. Li and J. Dudek, Phys. Rev. C **49**, R1250 (1994).
 - [4] S. Takami, K. Yabana, and M. Matsuo, Phys. Lett. B **431**, 242 (1998); M. Yamagami and K. Matsuyanagi, Nucl. Phys. A **672**, 123 (2000); M. Yamagami, K. Matsuyanagi, and M. Matsuo, Nucl. Phys. A **693**, 579 (2001).
 - [5] N. Schunck, J. Dudek, A. Gózdź, and P. H. Regan, Phys. Rev. C **69**, 061305(R) (2004).
 - [6] A. J. Sierk, Phys. Rev. C **33**, 2039 (1986).
 - [7] Ćwiok, J. Dudek, W. Nazarewicz, J. Skalski, and T. Werner, Comput. Phys. Commun. **46**, 379 (1987).
 - [8] N. Dubray, Ph.D. thesis, University of Strasbourg, 2005.
 - [9] J. Dobaczewski and P. Olbratowski, Comput. Phys. Commun. **158**, 158 (2004); **167**, 214 (2005); <http://www.fuw.edu.pl/~dobaczew/hfodd/hfodd.html>.
 - [10] C. W. Reich, Nuclear Data Sheets **99**, 753 (2003).